Resolving Ultrafast Photoinduced Deactivations in Water-Solvated Pyrimidine Nucleosides

Ana Julieta Pepino, Javier Segarra-Martí, Artur Nenov, Roberto Improta, and Marco Garavelli

***The Journal of Physical Chemistry Letters* 2017 *8* (8), 1777-1783**

The final published version is available online at : **http://dx.doi.org/10.1021/acs.jpclett.7b00316**

Resolving Ultrafast Photoinduced Deactivations in Water-solvated Pyrimidine Nucleosides

Ana Julieta Pepino,[a] Javier Segarra-Martí,[,b] Artur Nenov,[a] Roberto Improta,[*,c] and Marco Garavelli[*,a,b]*

[a]Dipartimento di Chimica Industriale "Toso Montanari" Viale del Risorgimento, 4, 40136 Bologna, Italy.

[b]Univ Lyon, ENS de Lyon, CNRS, Université Lyon 1, Laboratoire de Chimie UMR 5182, F-69342 Lyon, France.

[c]Istituto di Biostrutture e Bioimmagini CNR, Via Mezzocannone 16, I-80134 Napoli, Italy.

AUTHOR INFORMATION

Corresponding Author

E-mail: marco.garavelli@unibo.it.

E-mail: robimp@unina.it

E-mail: javier.segarra-marti@ens-lyon.fr

ABSTRACT. For the first time, ultrafast deactivations of photo-excited water-solvated pyrimidine nucleosides are mapped employing hybrid QM(CASPT2)/MM(AMBER) optimizations that account for explicit solvation, sugar effects and dynamically correlated potential energy surfaces. Low energy S_1/S_0 ring-puckering and ring-opening conical intersections (CIs) are suggested to drive the ballistic coherent sub-ps (<200fs) decays observed in each pyrimidine, the energetics controlling this processes correlating with the lifetimes observed. A second bright $^1\pi_2\pi^*$ state, promoting excited-state population branching and leading towards a third CI with the ground state, is proposed to be involved in the slower ultrafast decay component observed in Thd/Cyd. The transient spectroscopic signals of the competitive deactivation channels are computed for the first time. A general unified scheme for ultrafast deactivations, spanning the sub-to-few ps time domain, is eventually delivered, with computed data that matches the experiments and elucidates the intrinsic photo-protection mechanism in solvated pyrimidine nucleosides.

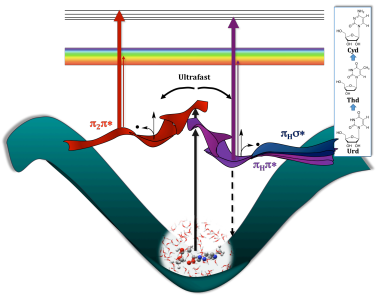

The ability of nucleobases to absorb in the 240–290 nm range and their intrinsic photostability, owing to the efficient conversion of radiative to kinetic energy via non-harmful radiationless pathways, is a well known and long studied topic.[1–16] Different time-resolved experiments and simulations have revealed intricate excited state dynamics spanning multiple time-scales, including ultrafast sub-ps decay components observed both *in vacuo*[5–9]

and in solution.[13–16] According to most of the available studies, these ultrafast features are mainly associated to the HOMO (H) to LUMO (L) ππ* transitions. However, several key issues, including the involvement of additional ππ* states (especially for purine) and/or dark nπ* transitions in the ultrafast dynamics are still matter of a lively debate.[17,18] There are several methodological bottlenecks preventing a complete elucidation of the photoactivated dynamics of nucleobases. The accuracy of the potential energy surface (PES) computed in solution is surely an important issue. At the same time, the assignment of time resolved experiments requires reliable simulations of the spectral signatures of all the excited states potentially involved in the photoinduced dynamics. In this contribution we make two important steps in this direction. On the one hand, for the first time, we have implemented a hybrid QM/MM scheme that couples a state-of-the-art *ab initio* multireference dynamically correlated description (CASPT2) of the photoactive moiety (the nucleobase) with an explicit classical atomistic model (AMBER force field) of the environment (sugar substituents and solvent). CASPT2/MM energies and gradients are then used to fully characterize (optimizing stationary points like minima, transition states and conical intersections, and connecting them with minimum energy paths) the decay channels associated to the two lowest energy ππ* excited states of water-solvated pyrimidine nucleosides (i.e. the biologically relevant species in the biologically relevant environment): deoxy-Thymidine (Thd), oxy-Uridine (Urd) and oxy-Cytidine (Cyd), see Figure 1. On the other hand, transient absorption/emission and photoelectron signals, including fluorescence anisotropy, of the main stationary points are also modeled and directly compared to the experiments. This is possible because the applied methodology allows the description *on the same footing (and with experimental accuracy)* of the energies of all the photochemically and spectroscopically relevant states along all investigated paths, a so far unreachable goal. Our analysis, besides providing the most

accurate characterization to date for these systems, unveils the role played in the ultrafast photoactivated dynamics by the second bright ππ* ($^1\pi_2\pi^*$) state and ring-opening conical intersections (CIs) that do also provide a competitive funnel for efficient non-radiative excited-state decay and, thus contribute the efficient photoprotection mechanisms observed in DNA/RNA. New experiments are eventually suggested to track these channels.

MM simulations and a cluster analysis are firstly performed, yielding two different clusters A and B (Fig. 1) that differ in the presence (syn) or absence (anti) of the intramolecular hydrogen bond between the 5' O−H Hydrogen of the ribose and the O7 heteroatom of the pyrimidine moiety, respectively. The structure closest to the centroid of cluster A (syn), holding ~65% of the total population, is selected as the starting point for our QM/MM simulations (see section S1 in the SI and ref. 16).

Vertical excitation energies and oscillator strengths for Urd, Thd and Cyd allow to assign the lowest-energy spectroscopic state to the H→L transition (S_1, $^1\pi_H\pi^*$), (4.64, 4.70 and 4.64 eV, respectively) while a second bright H-1→L state appears in all pyrimidines (S_3, $^1\pi_2\pi^*$) ~1 eV higher in energy (5.82, 5.88 and 5.57 eV, respectively) (See table S5 in the ESI). Dark nπ* states (S_2) systematically appear between the two bright states. Differences in excitation energy and energetic order appear when comparing solution and gas phase[5,6] results, that are explained in terms of ground and excited state dipole moments, as well as the diverse hydrogen bonding sensitivity, as already extensively discussed in the literature (see refs 13–15,17,19–23).

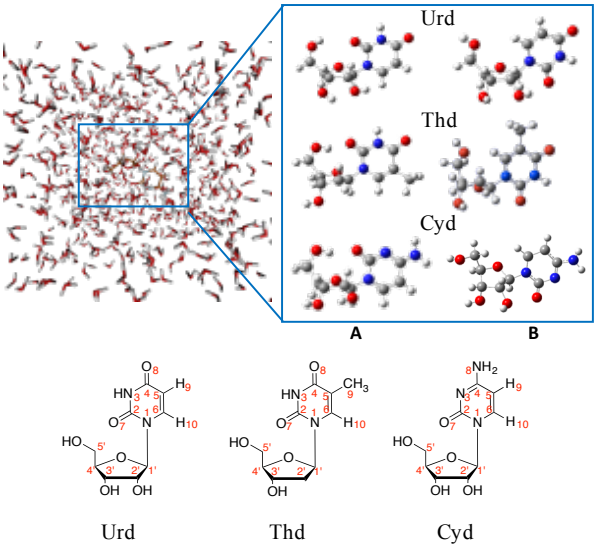

Figure 1. Main configurations (A and B) along the MM dynamics run obtained through RMS deviation cluster analysis for oxy-Uridine (Urd), deoxy-Thymidine (Thd) and oxy-Cytidine (Cyd). A detailed analysis is given in the SI.

S_3 corresponds to a bright ππ* state ($^1\pi_2\pi^*$) in all systems but, while in Urd and Thd this state is well separated lying about ~0.7 eV above S_2 ($^1n_O\pi^*$), in Cyd S_2 ($^1n_N\pi^*$, involving the electron lone pair on N3) and S_3 ($^1\pi_2\pi^*$) are degenerate (5.54 and 5.57 eV, respectively) at the FC region. It is also worth noting that, whereas relatively large energy differences can be observed at the FC region, once accounting semi classically for the vibrational broadening of the states and obtaining the cross-section (see Fig. 2), a sizable population of $^1\pi_2\pi^*$ can take place by direct excitation in Thd and Cyd (5% and 20% of the computed structures, respectively), whereas none is observed for Urd (these values refer to absorption at 267nm, i.e. 4.64 ± 0.1eV, matching the experimental excitation wavelength).

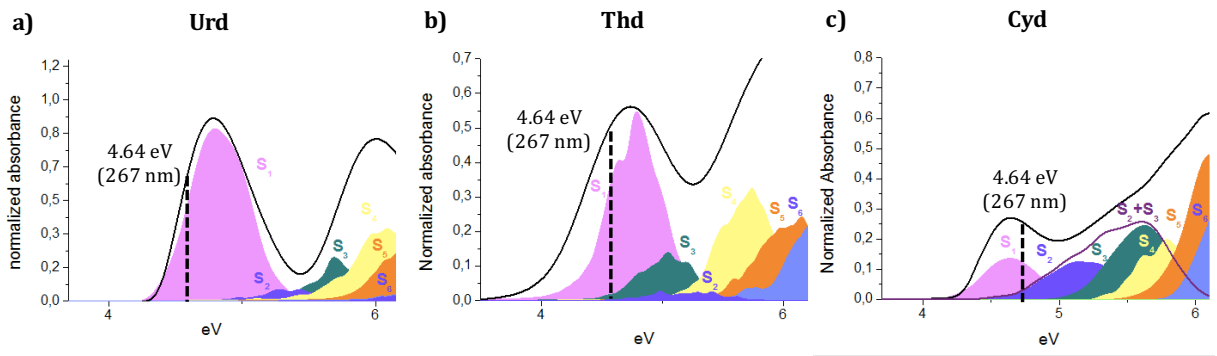

Figure 2. Absorption cross-sections computed at the MS-CASPT2/MM level for the pyrimidine nucleosides employing a Wigner distribution where 500 geometries were generated, as implemented in JADE.[24] Further details are given in the SI.

Figure 3 shows the computed deactivation routes for all solvated pyrimidine nucleosides. After photoexcitation to the bright S_1 ($^1\pi_H\pi^*$) state (purple solid line in Fig. 3), a steep path leads to a *planar* shallow minimum ($^1\pi_H\pi^*_{min\text{-}pl}$).[6,14,15,20] and then to a lower lying slightly puckered/twisted or "boat-like"[22] minimum ($^1\pi_H\pi^*_{min\text{-}tw}$) (see SI). The existence of a $^1\pi_H\pi^*_{min\text{-}pl}$-$^1\pi_H\pi^*_{min\text{-}tw}$ plateau correlates well with the broad experimentally observed emission and its band origin[25,26] in terms of vertical and adiabatic emissions (see Table S5 and Fig. 3). By proceeding along the puckering coordinate, the so-called ethylenic CI ($^1\pi_H\pi^*/S_0)_{CI}$ is eventually accessed overcoming a transition state ($^1\pi_H\pi^*_{min\text{-}tw}\rightarrow CI_{\pi H\pi^*/S0})_{TS}$ that is here optimized for the first time, thus allowing for a precise estimate in water of the energy barrier involved along this path (0.09, 0.12 and 0.15 eV for Urd, Thd and Cyd, respectively).

Notably, an additional deactivation pathway along S_1 exists (blue line in Figure 3), leading to the 'ring-opening' CI ($^1\pi_H\sigma^*/S_0)_{CI}$ recently reported in gas-phase[6,27,28]. In the CI region the S_1 state is described by a transition from the HOMO to a σ antibonding orbital located in the N1-C2 bond (labelled $\pi_H\sigma^*$ further on, see MOs description in the SI), and possesses a

zwitterionic character that involves a charge reorganization in the ring (see SI). A similar path was suggested by Gonzalez *and coworkers*[28] to be possible in Uracil, based on nonadiabatic CASSCF dynamics in gas-phase. Here we show that this route exists in all pyrimidines and is strongly stabilized in polar solvents, becoming more competitive than in gas-phase: $(^1\pi_H\sigma^*/S_0)_{CI}$ is almost degenerate to the ethylenic CI and involves similar energy barriers and a similar trend (0.14, 0.18 and 0.24 eV for Urd, Thd and Cyd, respectively, see also Table 1). Moreover, its formation comprises small geometrical changes (even smaller than the "ethylenic" path for Urd and Thd, see mass-weighted coordinates in Figure 3). All these arguments call for the ethylenic and ring-opening funnels as the main ultrafast $S_1 \rightarrow S_0$ decay regions in solvated pyrimidines. Very remarkably, the values and trend in the computed energy barriers (see Table 1) uphold the ultrafast rates registered with either fs-fluorescence up-conversion (FU) (~100, 150 and 200 fs lifetimes for solvated uracil, deoxy-Thd and deoxy-Cyd, respectively)[22,29] or fs-transient absorption (TA) experiments (deoxy-Urd: 210 fs,[25] oxy-Thd: 540 fs, and deoxy-Cyd: 720 fs),[30] further supporting this view. It is worth noting that CASPT2/MM transition state optimizations provide the most accurate estimates to date for the barriers to reach these two decay regions in water.

Following initial population of $\pi_H\pi^*$ upon absorption, the $\pi_2\pi^*$ state can also be accessed non-adiabatically through the $(^1\pi_H\pi^*/^1\pi_2\pi^*)_{CI}$ given its close proximity to the FC region (see Fig. 3). Upon either direct (for Thd and Cyd, see Fig. 2) or indirect (non-adiabatic) population, $\pi_2\pi^*$ is expected to decay towards its minimum $^1\pi_2\pi^*_{min}$ which is predicted to emit vertically at ~4 eV (see Table S5). However, emission intensity from $^1\pi_2\pi^*_{min}$ is rather weak and, for Urd and Thd, much smaller than that of $^1\pi_H\pi^*_{min}$. This feature could explain why this channel has not been detected in previous fs-FU experiments in deoxy-pyrimidines.[29] Once reaching the $^1\pi_2\pi^*_{min}$, a barrier (~0.88 and 0.24 eV for Urd and Thd,

respectively) has to be surmounted in order to reach the CI with S_0 ($^1\pi_2\pi^*/GS)_{CI}$ and decay non-radiatively. Given the high energy barrier in Urd, the easiest decay path would be a re-cross back to the $\pi_H\pi^*$ state. On the other hand, this channel may play a role in Thd due to the smaller barrier towards $(^1\pi_2\pi^*/GS)_{CI}$. We thus propose that the additional $\pi\pi^*$ deactivation channel recently tracked by time-resolved photoelectron spectra (TR-PES) in deoxy-Thd[17,31] is associated to $^1\pi_2\pi^*$ and not to $^1\pi_H\pi^*$ (see below).

As opposed to Thd and Urd, Cyd displays near-degeneracy between $^1\pi_2\pi^*_{min}$ and $(^1\pi_H\pi^*/^1\pi_2\pi^*)_{CI}$, thus suggesting efficient re-population of the $\pi_H\pi^*$ state. Accordingly, no signatures of the $^1\pi_2\pi^*$ state have been recorded by fs-FU experiments. However, relaxation on the $\pi_H\pi^*$ PES from $(^1\pi_H\pi^*/^1\pi_2\pi^*)_{CI}$ funnels the system towards a different minimum, $^1\pi_H\pi^*_{min\text{-}3}$, displaying different geometrical parameters compared to the other minima characterized (see SI), and a strong coupling with the $^1n_O\pi^*$ state. Its estimated vertical emission peaks at ~3.78 eV. This value falls within the range previously assigned to the emission signal of the ultrafast component, but it is anticipated here that its lower oscillator strength will difficult its experimental characterization. A transition state is optimized along the pathway connecting $^1\pi_H\pi^*_{min\text{-}3}$ and $(^1n_O\pi^*/^1\pi_H\pi^*/S_0)_{CI}$, displaying a moderate energy barrier of 0.32 eV. The decay is mediated in this case by a 3-state CI, previously reported by Kistler and Matsika[21] for gas phase cytosine, and that is highly coupled with the main carbonyl stretching motion behind this channel.

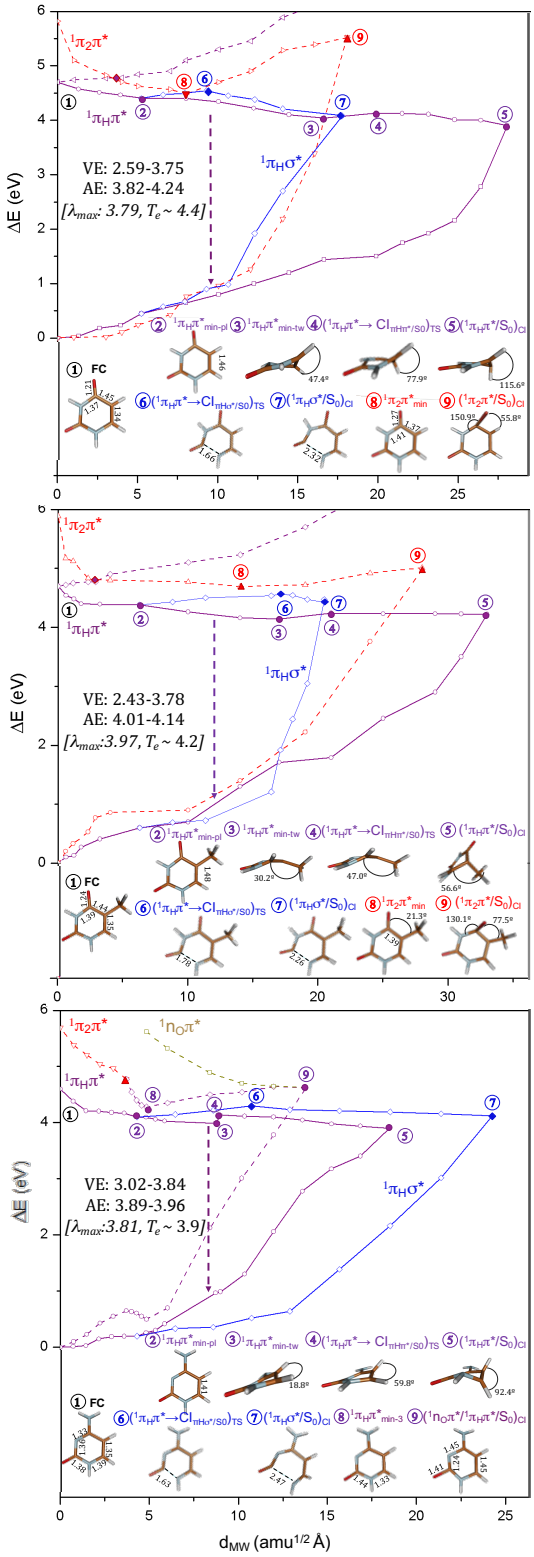

Figure 3. Evolution of the ground and lowest excited states for Urd (a), Thd (b) and Cyd (c) along the computed relaxation paths plotted in mass-weighted units. Full purple lines denote

the main ring-puckering CI channels, blue lines represent the ring-opening route and dotted lines depict the decay channels mediated by the $\pi_2\pi^*$. Computed vertical (VE) and adiabatic ZPE-corrected (AE) emissions are also reported together with the corresponding experimental values (in brackets).

Whereas Urd displays only a mono-exponential ultrafast decay on a <100 fs time scale,[25] time resolved fluorescence experiments show a bi-exponential excited state decay for deoxy-Thd,[29] and both oxy- and deoxy-Cyd,[32] with a fastest component <200 fs and an additional ultrafast yet slower sub- to few-ps component (0.7-1.8 ps, depending on the systems). It has been suggested that the shortest-lived component could be associated to the relaxation of the wave packet out of the FC region, while the second one would account for overcoming the barrier and finally decaying to the ground state.[7,15,22,33] However, it is apparent that the initial motion triggered upon absorption would mainly populate bond-stretching modes in a timescale of tens (rather than hundreds) of fs. Consistently, vibrational coherences have been recently probed along these modes in nucleobases,[34] while it has also been shown that full coherent photo-processes in similar biological systems can take place in a sub-50 fs regime.[35] Furthermore, time-resolved photoelectron spectroscopy (TR-PES) experiments on deoxy-Thd also find a bi-exponential decay (time components 120 and 390 fs) with evidence of two independent decay channels involving two different $\pi\pi^*$ states.[17] Keeping this in mind, and considering that only purposely tailored dynamical studies[9,36] coupled with correlated potential energy surfaces can provide a definitive assignment of the experimental time-components, this study strongly suggests to assign the fastest (<200 fs) decay component to direct $^1\pi_H\pi^* \rightarrow S_0$ ballistic decay for all pyrimidine nucleosides,[37] that is driven by the ethylenic and ring-opening CIs, whereas the second ultrafast component observed in Thd and Cyd would most likely arise from a fraction of the wave packet being slowed down due to

trapping either in a local minimum along the flat $^1\pi_H\pi^*$ PES, or in the $^1\pi_2\pi^*$ state, or to a combination of both.

It is worth noting that our model, involving MM water molecules, is unable to track proton transfer events between excited nucleobases and neighboring water molecules that have been previously suggested[38,39] as possible decay routes. Inclusion of QM waters in the current model is out of reach due to its computational cost. Moreover, one would have to account for several solvation layers in the QM region in order to include the likely proton diffusion event along the water hydrogen-bonding network as has been recently analyzed in similar systems.[40] Nevertheless, we expect the involvement of these processes to be minor in ultrafast decays, compared to those related to the bright and initially accessed $\pi\pi^*$ states. Electron ejection from the excited base into water is yet another possibility that has been previously highlighted in the literature.[41] We have not considered this path in the present study as it has sizable contributions only at high energies (~220nm, UV-C), whereas our study focuses on the deactivation channels in the biologically relevant sunlight UV-A/B spectral range (280-400 nm), which is the one employed in the time-resolved experiments we compare our simulations to.

The increasing energy barriers to the S_1/S_0 funnels (and, hence, longer lifetimes) are expected to correlate with increasing fluorescence quantum yields (QY). Despite featuring the highest barrier, though, Cyd displays an intermediate fluorescence QY with respect to Thd and Urd ($0.89\text{x}10^{-4}$ and $1.02\ \text{x}10^{-4}$ for oxy and deoxy-Cyd, respectively,[29,32] see Table 1). This can be only understood/comprehended in the scope of the more complex deactivation mechanism in Cyd, involving both the $^1\pi_H\pi^*$ and the $^1\pi_2\pi^*$ states. While the oscillator strength does not change significantly along the $^1\text{H}\pi^*$ state ($f(^1\pi_H\pi^*_{\text{min-pl}})/f(^1\pi_H\pi^*_{\text{FC}})$: 0.96; $f(^1\pi_H\pi^*_{\text{min-}}$

$_{tw}$)/f($^1\pi_H\pi^*_{FC}$): 0.93), thus making the fluorescence QY along this channel dependent only on the barriers, its decrease is stronger along the $^1\pi_2\pi^*$ relaxation path (f($^1\pi_H\pi^*_{min\text{-}3}$)/$f$($^1\pi_2\pi^*_{FC}$): 0.52). Thus, with increasing significance of the $^1\pi_2\pi^*$ deactivation channel larger fractions of the population are rerouted to the ($^1\pi_H\pi^*$)$_{min\text{-}3}$ minimum with reduced emission. In that way, the broken correlation between excited state lifetimes and fluorescence QY indirectly supports the involvement of the $^1\pi_2\pi^*$ state in the deactivation mechanism of Cyd.

Table 1. Fluorescence Quantum Yield, Energy barrier, lifetime and the ratio between the oscillator strengths f of the bright states in the FC and in the $\pi_H\pi^*$ minima for Urd, Thd and Cyd.

		Urd	Thd	Cyd
Fluorescence Quantum Yield (QY, 10^{-4})[29,32]		0.4	1.32	0.89
Energy Barrier (eV)	**Ethene-like**	0.09	0.12	0.15
	Open-ring	0.14	0.18	0.24
Lifetime (ps)		0.10	0.15	0.20
f($^1\pi_H\pi^*_{min\text{-}pl}$)/$f$($^1\pi_H\pi^*_{FC}$)		0.73	0.90	0.96
f($^1\pi_H\pi^*_{min\text{-}tw}$)/$f$($^1\pi_H\pi^*_{FC}$)		0.70	0.88	0.93
f($^1\pi_H\pi^*_{min\text{-}3}$)/$f$($^1\pi_2\pi^*_{FC}$)		-	-	0.52

In order to assign the available spectroscopic results to the corresponding decay pathways, the spectral fingerprints (emission, fluorescence anisotropy, excited state absorptions (ESAs) and photoelectron signals) out of the stationary points described in this work have been systematically computed and compared face-to-face with the available experimental data.

The computed fluorescence anisotropy[29,42,43] values at time zero (r_0) are reported in the SI and compared with experiments. Though this technique can in principle ascertain if the nature of the absorbing and emitting states is different, in our case is not very informative. In particular, initial excitation to the $^1\pi_2\pi^*$ state in Cyd and subsequent emission from $^1\pi_H\pi^*_{min\text{-}3}$ reached after re-population of the $^1\pi_H\pi^*$ state, as previously suggested, yield analogous anisotropy values as those reported when accessing the $^1\pi_H\pi^*$ state (either planar/twisted $^1\pi_H\pi^*$ minima) directly upon excitation, thus showing how this observable is incapable of

disentangling these two different decay routes. In Thd, however, a second decay mechanism along the $^1\pi_2\pi^*$ state is also proposed, leading to $^1\pi_2\pi^*_{min}$ whose computed r_0 is quite different from the one obtained along the $^1\pi_H\pi^*$ decay. This result suggests that these two decay channels could be differentiated by the experiments, at least in Thd. However, the anisotropy was measured at 330 nm, being out of range for any kind of $\pi_2\pi^*$ emissive contribution that is predicted to fall at more blue shifted energies (~300 nm).

TR-Transient Absorption is one of the most powerful methods to characterize excited state dynamics. It has been extensively used in fs-TA experiments on oligonucleotides in order to fit the lifetimes and disentangle different decay channels. Indeed, due to the different electronic structure of each photoactive state, a specific ESA is expected that is thus able to provide an indirect signature of its population. Unfortunately, up to now, no computational study of ESA in solution was available, making more difficult the assignment of the experimental spectra. Here we report first efforts in computing ESA signals on top of the different key $\pi\pi^*$ minima (see Fig. 4) and provide a direct comparison with the experimental evidence under the assumption that the ESAs of the individual $\pi\pi^*$ states are dominated by the electronic structure at their corresponding minima. Figure 4, bottom panels, reports a breakdown of the ESA spectrum of each nucleoside into its contributions. In a nutshell, all three systems show two distinct contributions: a) a strong ESA in the near-UV between 300 nm – 450 nm, arising mainly from ESA of the planar minima, except for Urd where both $\pi_H\pi^*_{min\text{-}pl}$ and $\pi_H\pi^*_{min\text{-}tw}$ contribute equally in this spectral region; this suggests that ultrafast decays may also be followed in the UV range; b) a less intense ESA in the visible between 500 nm – 650 nm that can be assigned to populating the twisted $\pi_H\pi^*$ conformations. Notably, the $\pi_H\pi^*_{min\text{-}3}$ minimum found in Cyd and associated with depopulating the $\pi_2\pi^*$ state exhibits a pronounced absorption in this window which can be used to target its

photophysics. The reported visible signatures are in a good agreement with those recorded for the ultrafast $\pi_H\pi^*$-mediated decay channels.[30] It should be noted though that, due to their broad unstructured line shapes, ESAs are not well-suited for the unambiguous disentanglement of the individual channels and it should be considered that the multiple lifetimes fitted for these signals at selected wavelengths are more probably associated with the dynamics in simultaneously populated channels rather then a single channel subject to a multi-exponential decay mechanism, as often considered. Indeed, and notably, these signals do also appear along the $^1\pi_2\pi^*$ and $^1\pi_H\sigma^*$ deactivation routes (the latter sharing the same planar $^1\pi_H\pi^*$ minimum - $\pi_H\pi^*_{min\text{-}pl}$ - of the $\pi_H\pi^*$ pathways), and are thus unable to distinguish the different channels.

Another way to track photoinduced phenomena is based on TR-PES, where the average kinetic energy (AKE) of the ejected electrons is registered. This magnitude is related to the excess energy between the probe pulse employed and the energy gap between the initially accessed singlet and cationic state (D_n) generated. AKEs for the different key structures are estimated and shown in Figure 4. The study by Buchner *et al.*[17] is taken as a reference and is extended using a larger active space and basis set: all values displayed refer to the 267-nm pump and 238-nm probe set-up described therein enabling photoionization in nucleosides (up to 9.85 eV, cationic states having been rescaled to match the experimental value reported in the literature for Cyd and Thd,[44] Urd being considered to be in the same range; see SI). Urd and Thd feature their largest AKEs at the vicinities of the FC region, where the S_1-D_0 gap is the smallest. This correlates with what has been reported in the literature for deoxy-Thd[17] and for deoxy-nucleotides[45] *in vacuo* with 400-nm probe pulses where the largest AKEs are registered at earlier times. Slightly lower values are obtained for $^1\pi_2\pi^*_{min}$, in agreement with Buchner *et al.*[17] that indeed register lower AKEs for the second sub-ps channel in deoxy-Thd.

This result strongly supports the assignment of this decay channel to the $^1\pi_2\pi^*$ state and the importance of including this state in the theoretical treatment. It is worth noting that contributions along the ultrafast $^1\pi_H\pi^*$ state are here predicted to decay rapidly, practically vanishing already at $^1\pi_H\pi^*_{min\text{-}tw}$ with estimates AKE ~0.4 eV, evidencing a larger singlet to doublet gap along the pathway that is expected to difficult the proper monitoring of the excited state dynamics under the conditions here considered.[17] More energetic vacuum UV (VUV) probe pulses may provide an alternative, and ultimate, technique for a definitive answer.[46] Cyd presents the only case where one of its minima $^1\pi_H\pi^*_{min\text{-}3}$ displays larger AKEs than the FC region, being a good probe for this channel and its involvement in the overall photo-process. While no experimental time-resolved study has been found for this specific system, we predict the S_1-D_0 gap to remain small enough to be probed along the shortest-lived component, which makes TR-PES a very appealing technique for tracking the ultrafast events in Cyd.

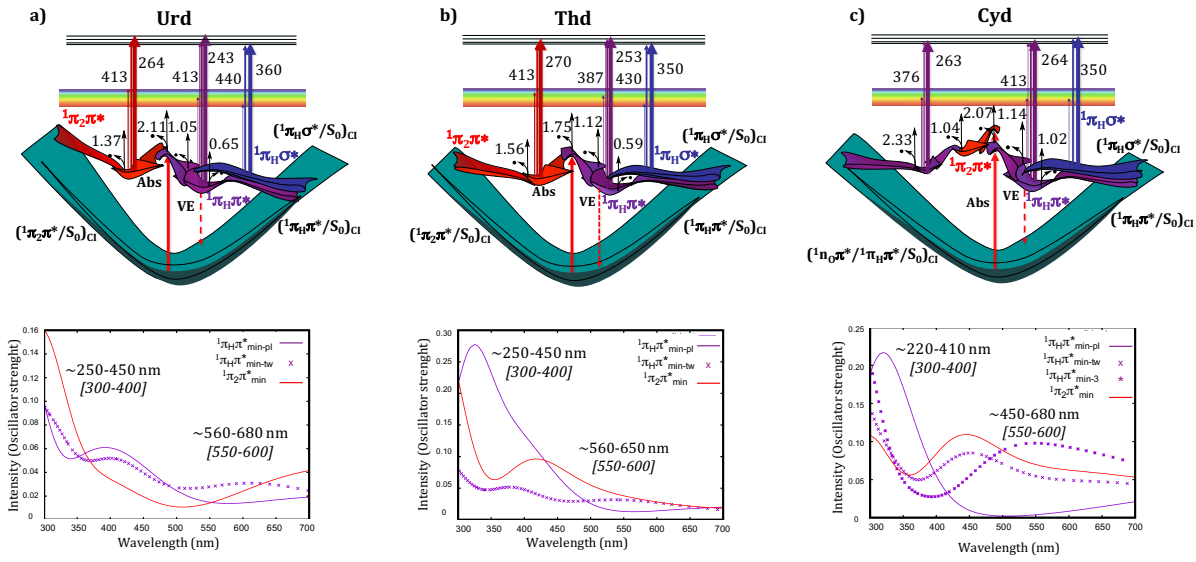

Figure 4. Diagram containing the photochemically relevant mechanisms in water-solvated Urd (a), Thd (b) and Cyd (c) and their related spectroscopic fingerprints. The colored arrows denote excited state absorptions (ESAs), their thickness representing their relative intensity

(computed values in nm). The corresponding calculated ESA spectra in nm in the bottom panels (computed ranges are reported together with the corresponding experimental values in brackets). Black arrows correspond to Average Kinetic Energies (AKEs) in eV.

In conclusion, by employing QM(CASPT2)/MM energies and gradients with explicit solvation and realistic systems, we have described all the ultrafast (sub- to few-ps) decay paths in water solvated pyrimidine nucleosides and report a complete and coherent (static) picture. Corresponding spectroscopic signals (spanning transient absorption/emission, fluorescence anisotropy and photoelectron) have also been systematically modeled and compared face-to-face with available observations to support experimental assignments. Our study supports a ballistic coherent ultrafast decay of the bright lowest-lying $^1\pi_H\pi^*$ state mediated by two possible CIs on the shortest sub-ps lifetimes and postulates a new scenario where the existence of a second accessible $^1\pi_2\pi^*$ state in Cyd/Thd could potentially account for the second component registered experimentally in the sub- to few-ps regime in these species. Given the limitations of present spectroscopic methods, more extensive theoretical and experimental studies like the TR-PES experiments suggested above and those involving multidimensional electronic spectroscopy[47,48] are thus required for a final assignment, particularly so in Cyd. It is also worth to stress that longer-living decay channels (tens of ps to ns), also registered experimentally in solution and possibly involving other paths and states (e.g., base to sugar proton transfers,[49,50] $n\pi^*$ dark states[51] triplet states[52]), are not considered here and will be the focus of a forthcoming study.

Eventually, this work delivers a fundamental step towards a full understanding of ultrafast decay in solvated pyrimidines and their spectral signals. The unified mechanistic scheme

presented here calls for a common evolutionary origin and path under the pressure of natural selection in the vital quest for optimal DNAR/RNA photo-protection.[53,54]

ACKNOWLEDGEMENTS

M.G. acknowledges support by the European Research Council Advanced Grant STRATUS (ERC-2011-AdG No.291198) and of the French Agence National de la Recherche (FEMTO-2DNA, ANR-15-CE29-0010). J.S.-M. acknowledges project no. CTQ2014-58624-P of the Spanish MINECO. R.I. thanks Dr. L. Martínez-Fernández for useful discussions and CNR/CNRS Progetto Bilaterale 2015 for financial support.

REFERENCES

(1) Kleinermanns, K.; Nachtigallová, D.; de Vries, M. S. Excited State Dynamics of DNA Bases. *Int. Rev. Phys. Chem.* **2013**, *32* (2), 308–342.

(2) Chen, J.; Kohler, B. Base Stacking in Adenosine Dimers Revealed by Femtosecond Transient Absorption Spectroscopy. *J. Am. Chem. Soc.* **2014**, *136* (17), 6362–6372.

(3) Crespo-Hernández, C. E.; Cohen, B.; Hare, P. M.; Kohler, B. Ultrafast Excited-State Dynamics in Nucleic Acids. *Chem. Rev.* **2004**, *104* (4), 1977–2019.

(4) Middleton, C. T.; de La Harpe, K.; Su, C.; Law, Y. K.; Crespo-Hernández, C. E.; Kohler, B. DNA Excited-State Dynamics: From Single Bases to the Double Helix. *Annu. Rev. Phys. Chem.* **2009**, *60* (1), 217–239.

(5) Giussani, A.; Segarra-Martí, J.; Roca-Sanjuán, D.; Merchán, M. No Title. *Top. Curr. Chem.* **2013**, *355*, 57–97.

(6) Barbatti, M.; Borin, A. C.; Ullrich, S. Photoinduced Processes in Nucleic Acids. In *Photoinduced Phenomena in Nucleic Acids I: Nucleobases in the Gas Phase and in Solvents*; Barbatti, M., Borin, C. A., Ullrich, S., Eds.; Springer International

Publishing: Cham, 2015; pp 1–32.

(7) Improta, R.; Santoro, F.; Blancafort, L. Quantum Mechanical Studies on the Photophysics and the Photochemistry of Nucleic Acids and Nucleobases. *Chem. Rev.* **2016**, *116* (6), 3540–3593.

(8) Mai, S.; Richter, M.; Marquetand, P.; González, L. Excitation of Nucleobases from a Computational Perspective II: Dynamics. In *Photoinduced Phenomena in Nucleic Acids I: Nucleobases in the Gas Phase and in Solvents*; Barbatti, M., Borin, C. A., Ullrich, S., Eds.; Springer International Publishing: Cham, 2015; pp 99–153.

(9) Barbatti, M.; Aquino, A. J. a; Szymczak, J. J.; Nachtigallová, D.; Hobza, P.; Lischka, H. Relaxation Mechanisms of UV-Photoexcited DNA and RNA Nucleobases. *Proc. Natl. Acad. Sci. U. S. A.* **2010**, *107* (50), 21453–21458.

(10) Markovitsi, D.; Gustavsson, T.; Talbot, F. Excited States and Energy Transfer among DNA Bases in Double Helices. *Photochem. Photobiol. Sci.* **2007**, *6* (7), 717–724.

(11) Markovitsi, D.; Gustavsson, T.; Vayá, I. Fluorescence of DNA Duplexes: From Model Helices to Natural DNA. *J. Phys. Chem. Lett.* **2010**, *1* (22), 3271–3276.

(12) Gustavsson, T.; Improta, R.; Markovitsi, D. DNA/RNA: Building Blocks of Life under UV Irradiation. *J. Phys. Chem. Lett.* **2010**, *1* (13), 2025–2030.

(13) Santoro, F.; Barone, V.; Gustavsson, T.; Improta, R. Solvent Effect on the Singlet Excited-State Lifetimes of Nucleic Acid Bases: A Computational Study of 5-Fluorouracil and Uracil in Acetonitrile and Water. *J. Am. Chem. Soc.* **2006**, *128* (50), 16312–16322.

(14) Mercier, Y.; Santoro, F.; Reguero, M.; Improta, R. The Decay from the Dark Nπ* Excited State in Uracil: An Integrated CASPT2/CASSCF and PCM/TD-DFT Study in the Gas Phase and in Water. *J. Phys. Chem. B* **2008**, *112* (35), 10769–10772.

(15) Improta, R.; Barone, V. The Excited States of Adenine and Thymine Nucleoside and Nucleotide in Aqueous Solution: A Comparative Study by Time-Dependent DFT Calculations. *Theor. Chem. Acc.* **2008**, *120* (4-6), 491–497.

(16) Altavilla, S. F.; Segarra-Martí-, J.; Nenov, A.; Conti, I.; Rivalta, I.; Garavelli, M. Deciphering the Photochemical Mechanisms Describing the UV-Induced Processes Occurring in Solvated Guanine Monophosphate. *Front. Chem.* **2015**, *3*, 1–12.

(17) Buchner, F.; Nakayama, A.; Yamazaki, S.; Ritze, H. H.; Lübcke, A. Excited-State Relaxation of Hydrated Thymine and Thymidine Measured by Liquid-Jet Photoelectron Spectroscopy: Experiment and Simulation. *J. Am. Chem. Soc.* **2015**, *137* (8), 2931–2938.

(18) Segarra-Martí, J.; Francés-Monerris, A.; Roca-Sanjuán, D.; Merchán, M. Assessment of the Potential Energy Hypersurfaces in Thymine within Multiconfigurational Theory: CASSCF vs. CASPT2. *Molecules* **2016**, *21* (12), 1666.

(19) Giussani, A.; Segarra-Martí, J.; Nenov, A.; Rivalta, I.; Tolomelli, A.; Mukamel, S.; Garavelli, M. Spectroscopic Fingerprints of DNA/RNA Pyrimidine Nucleobases in Third-Order Nonlinear Electronic Spectra. *Theor. Chem. Acc.* **2016**, *135* (5), 1–18.

(20) Zhang, X.; Herbert, J. M. Excited-State Deactivation Pathways in Uracil versus Hydrated Uracil: Solvatochromatic Shift in the 1nπ* State Is the Key. *J. Phys. Chem. B* **2014**, *118* (28), 7806–7817.

(21) Kistler, K. A.; Matsika, S. Solvatochromic Shifts of Uracil and Cytosine Using a Combined Multireference Configuration Interaction/molecular Dynamics Approach and the Fragment Molecular Orbital Method. *J. Phys. Chem. A* **2009**, *113* (45), 12396–12403.

(22) Gustavsson, T.; Bányász, Á.; Lazzarotto, E.; Markovitsi, D.; Scalmani, G.; Frisch, M.

J.; Barone, V.; Improta, and R. Singlet Excited-State Behavior of Uracil and Thymine in Aqueous Solution: A Combined Experimental and Computational Study of 11 Uracil Derivatives. *J. Am. Chem. Soc.* **2006**, *128* (2), 607–619.

(23) Martínez, L.; Pepino, A. J.; Segarra-mart, J.; Banyasz, A.; Garavelli, M.; Improta, R. Computing the Absorption and Emission Spectra of 5‑Methylcytidine in Different Solvents : A Test-Case for Di Ff Erent Solvation Models. *J. Chem. Theory Comput.* **2016**, *12*, 4430–4439.

(24) Du, L.; Lan, Z. An on-the-Fly Surface-Hopping Program Jade for Nonadiabatic Molecular Dynamics of Polyatomic Systems: Implementation and Applications. *J. Chem. Theory Comput.* **2015**, *11* (4), 1360–1374.

(25) Cohen, B.; Crespo-Hernández, C. E.; Kohler, B.; Crespo-Hernandez, C. E.; Kohler, B. Strickler-Berg Analysis of Excited Singlet State Dynamics in DNA and RNA Nucleosides. *Faraday Discuss.* **2004**, *127* (0), 137–147.

(26) Peon, J.; Zewail, A. H. DNA/RNA Nucleotides and Nucleosides: Direct Measurement of Excited-State Lifetimes by Femtosecond Fluorescence up-Conversion. *Chem. Phys. Lett.* **2001**, *348* (3-4), 255–262.

(27) Nachtigallová, D.; Aquino, A. J. A.; Szymczak, J. J.; Barbatti, M.; Hobza, P.; Lischka, H. Nonadiabatic Dynamics of Uracil: Population Split among Different Decay Mechanisms. *J. Phys. Chem. A* **2011**, *115* (21), 5247–5255.

(28) Richter, M.; Mai, S.; Marquetand, P.; González, L. Ultrafast Intersystem Crossing Dynamics in Uracil Unravelled by Ab Initio Molecular Dynamics. *Phys. Chem. Chem. Phys.* **2014**, *16* (44), 24423–24436.

(29) Onidas, D.; Markovitsi, D.; Marguet, S.; Sharonov, A.; Gustavsson, T. Fluorescence Properties of DNA Nucleosides and Nucleotides: A Refined Steady-State and

Femtosecond Investigation. *J. Phys. Chem. B* **2002**, *106* (43), 11367–11374.

(30) Pecourt, J. M. L.; Peon, J.; Kohler, B. DNA Excited-State Dynamics: Ultrafast Internal Conversion and Vibrational Cooling in a Series of Nucleosides. *J. Am. Chem. Soc.* **2001**, *123* (42), 10370–10378.

(31) Nakayama, A.; Harabuchi, Y.; Yamazaki, S.; Taketsugu, T. Photophysics of Cytosine Tautomers: New Insights into the Nonradiative Decay Mechanisms from MS-CASPT2 Potential Energy Calculations and Excited-State Molecular Dynamics Simulations. *Phys. Chem. Chem. Phys.* **2013**, *15* (29), 12322–12339.

(32) Ma, C.; Cheng, C. C.; Chan, C. T.; Chan, R. C.; Kwok, W. Remarkable Effects of Solvent and Substitution on the Photo-Dynamics of Cytosine : A Femtosecond Broadband Time-Resolved Fluorescence and. *Phys. Chem. Chem. Phys.* **2015**, *17*, 19045–19057.

(33) Rottger, K.; Marroux, H.; Bohnke, H.; Morris, D.; Voice, A.; Temps, F.; Roberts, G. M.; Orr-Ewing, A. Probing the Excited State Relaxation Dynamics of Pyrimidine Nucleosides in Chloroform Solution. *Faraday Discuss.* **2016**, *194*, 683–708.

(34) Xue, B.; Yabushita, A.; Kobayashi, T. Ultrafast Dynamics of Uracil and Thymine Studied Using a Sub-10 Fs Deep Ultraviolet Laser. *Phys. Chem. Chem. Phys.* **2016**, *18* (25), 17044–17053.

(35) Johnson, P. J. M.; Halpin, A.; Morizumi, T.; Prokhorenko, V. I.; Ernst, O. P.; Miller, R. J. D. Local Vibrational Coherences Drive the Primary Photochemistry of Vision. *Nat. Chem.* **2015**, *7* (12), 980–986.

(36) Richter, M.; Marquetand, P.; González-Vázquez, J.; Sola, I.; González, L. Femtosecond Intersystem Crossing in the DNA Nucleobase Cytosine. *J. Phys. Chem. Lett.* **2012**, *3* (21), 3090–3095.

(37) Merchán, M.; González-Luque, R.; Climent, T.; Serrano-Andrés, L.; Rodríguez, E.; Reguero, M.; Pel??ez, D. Unified Model for the Ultrafast Decay of Pyrimidine Nucleobases. *J. Phys. Chem. B* **2006**, *110* (51), 26471–26476.

(38) Barbatti, M. Photorelaxation Induced by Water-Chromophore Electron Transfer. *J. Am. Chem. Soc.* **2014**, *136* (29), 10246–10249.

(39) Wu, X.; Karsili, T. N. V; Domcke, W. Excited-State Deactivation of Adenine by Electron-Driven Proton-Transfer Reactions in Adenine-Water Clusters: A Computational Study. *ChemPhysChem* **2016**, *17* (9), 1298–1304.

(40) Shinobu, A.; Agmon, N. Proton Wire Dynamics in the Green Fluorescent Protein. *J Chem Theory Com* **2016**, *13* (1), 353–369.

(41) Roberts, G. M.; Marroux, H. J. B.; Grubb, M. P.; Ashfold, M. N. R.; Orr-Ewing, A. J. On the Participation of Photoinduced N-H Bond Fission in Aqueous Adenine at 266 and 220 Nm: A Combined Ultrafast Transient Electronic and Vibrational Absorption Spectroscopy Study. *J. Phys. Chem. A* **2014**, *118* (47), 11211–11225.

(42) Gustavsson, T.; Sharonov, A.; Onidas, D.; Markovitsi, D. Adenine, Deoxyadenosine and Deoxyadenosine 5′-Monophosphate Studied by Femtosecond Fluorescence Upconversion Spectroscopy. *Chem. Phys. Lett.* **2002**, *356* (1-2), 49–54.

(43) Gustavsson, T.; Sarkar, N.; Lazzarotto, E.; Markovitsi, D.; Improta, R. Singlet Excited State Dynamics of Uracil and Thymine Derivatives: A Femtosecond Fluorescence Upconversion Study in Acetonitrile. *Chem. Phys. Lett.* **2006**, *429* (4-6), 551–557.

(44) Slavíček, P.; Winter, B.; Faubel, M.; Bradforth, S. E.; Jungwirth, P. Ionization Energies of Aqueous Nucleic Acids: Photoelectron Spectroscopy of Pyrimidine Nucleosides and Ab Initio Calculations. *J. Am. Chem. Soc.* **2009**, *131* (18), 6460–6467.

(45) Chatterley, A. S.; West, C. W.; Stavros, V. G.; Verlet, J. R. R. Time-Resolved

Photoelectron Imaging of the Isolated Deprotonated Nucleotides. *Chem. Sci.* **2014**, *5*, 3963–3975.

(46) Horton, S.; Liu, Y.; Matsika, S.; Weinacht, T. Time-Resolved UV-Pump (4.8eV) and Vacuum-UV (8eV) Probe Experiments of Neutral Excited State Dynamics. In *47th Annual Meeting of the APS Division of Atomic, Molecular and Optical Physics*; 2016.

(47) Nenov, A.; Giussani, A.; Segarra-Martí, J.; Jaiswal, V. K.; Rivalta, I.; Cerullo, G.; Mukamel, S.; Garavelli, M. Modeling the High-Energy Electronic State Manifold of Adenine: Calibration for Nonlinear Electronic Spectroscopy. *J. Chem. Phys.* **2015**, *142* (21).

(48) Prokhorenko, V. I.; Picchiotti, A.; Miller, R. J. D. New Insight into Photophysics of DNA Nucleobases. **2016**, 4–6.

(49) Tuna, D.; Sobolewski, A. L.; Domcke, W. Mechanisms of Ultrafast Excited-State Deactivation in Adenosine. *J. Phys. Chem. A* **2014**, *118* (1), 122–127.

(50) Tuna, D.; Domcke, W. Excited-State Deactivation in 8-Oxo-Deoxyguanosine: Comparison between Anionic and Neutral Forms. *Phys. Chem. Chem. Phys.* **2016**, *18* (2), 947–955.

(51) Improta, R.; Santoro, F.; Blancafort, L. Quantum Mechanical Studies on the Photophysics and the Photochemistry of Nucleic Acids and Nucleobases. *Chem. Rev.* **2016**, *116* (6), 3540–3593.

(52) González-Luque, R.; Climent, T.; González-Ramírez, I.; Merchán, M.; Serrano-Andrés, L. Singlet−Triplet States Interaction Regions in DNA/RNA Nucleobase Hypersurfaces. *J. Chem. Theory Comput.* **2010**, *6* (7), 2103–2114.

(53) Serrano-Andrés, L.; Merchán, M. Are the Five Natural DNA/RNA Base Monomers a Good Choice from Natural Selection?. A Photochemical Perspective. *J. Photochem.*

Photobiol. C Photochem. Rev. **2009**, *10* (1), 21–32.

(54) Beckstead, A. A.; Zhang, Y.; Vries, S. De; Kohler, B. Life in the Light : Nucleic Acid Photoproperties as a. *Phys. Chem. Chem. Phys.* **2016**, *18*, 24228–24238.